Journal of Non-Crystalline Solids 447 (2016) 307–314

Contents lists available at ScienceDirect

Journal of Non-Crystalline Solids

journal homepage: www.elsevier.com/locate/jnoncrysol

Low-cost preparation of silica aerogel for optimized adsorptive removal of naphthalene from aqueous solution with central composite design (CCD)

A.R. Yaqubzadeh [a], A. Ahmadpour [a,*], T. Rohani Bastami [b], M.R. Hataminia [c]

[a] Department of Chemical Engineering, Faculty of Engineering, Ferdowsi University of Mashhad, Mashhad, Iran
[b] Department of Chemical Engineering, Faculty of Engineering, Quchan University of Advanced Technology, Quchan, P.O. Box 94771-67335, Iran
[c] Chemical Engineering Department, Sahand University of Technology, Sahand New Town, Tabriz, Iran

ARTICLE INFO

Article history:
Received 12 April 2016
Received in revised form 13 June 2016
Accepted 15 June 2016
Available online xxxx

Keywords:
Silica aerogel
Naphthalene
Adsorption
Design experiment
Response surface

ABSTRACT

Nanostructured silica aerogels are expensive porous materials with unique properties. Thus, the application of a cost-effective synthesis method will be highly effective for large-scale. Fourier transform infrared (FTIR) spectroscopy, scanning electron microscopy (SEM), BET surface area and contact angle and the density was determined by the pycnometry method. To investigate the adsorptive performance of silica aerogel, naphthalene pollutant was used as an organic pollutant model in the wastewater. In this study the process variables such as contact time, concentration of adsorbent, pH of solution and interaction of these variables in the adsorption process for the removal of the naphthalene from water by silica aerogel were evaluated. Furthermore, to achieve the predicted model and prepare the optimum condition of the process, the central composite design of the response surface methodology was utilized. According to the results of ANOVA table, a second order nonlinear model was obtained to predict the removal of naphthalene. The model adequacy was guaranteed by the assessment of statistical parameters such as coefficient of determination ($R^2 = 0.903$), adjusted R^2 (0.877) and adequate precision (19.23). In the kinetic study, the pseudo-second order model was consistent with the experimental results.

1. Introduction

Polycyclic aromatic hydrocarbons (PAHs) are chemical compounds with at least two rings, with some cases having up to 6 rings [1–3]. Chemical and physical properties of PAHs depend on the ring number and subsequently molecular weight (M_w). Compounds with low molecular weight have high reactivity and solubility in water [4]. However, based on their characteristics, the low molecular weight of PAHs imposes hazardous effects on human health compared to PAHs with high molecular weights [5]. People who are exposed to these water pollutants may be at cancer risk. PAHs can be produced in various industries such as coking plants, asphalt production, aluminum production, smokehouse, etc. [6–8]. As the smallest PAH with two benzene rings, naphthalene has the highest solubility and stability in water compared to all other forms of PAHs [9]. It often pollutes groundwater and surface waters in industrial cities due to the wastewater discharge [10]. The removal of naphthalene from wastewater has been the subject of many studies in which various methods have been used for this purpose. These methods include advanced oxidation process [11], chlorination [12], photocatalytic process [13,14], biodegradation [15,16], and adsorption [17–19]. Flexibility, convenient operation, low investment, low energy consumption and safety are the main features of adsorption process [20,21].

In the adsorption process, the suitable sorbent should have a number of characteristics like high specific surface area, high pore volume, suitable pore-size distribution, high thermal stability, easy regeneration process and low cost [22,23].

In the case of PAHs adsorption from wastewater, the hydrophobicity of surface is an important property of the adsorbent that reinforces high tendency of adsorbate to adsorbent. Naphthalene with two benzene rings is a non-polar molecule that can be properly treated with hydrophobic adsorbent. In this view, the silica aerogel as an adsorbent with hydrophobic surface can be suitable for the PAHs adsorption.

Silica aerogels are nanostructured solid materials with unique properties such as high porosity, high specific surface area, mesoporous structure, low thermal conductivity, high thermal stability and functionalization (surface modification) [24–26]. Additionally, they can be obtained in the form of monoliths, beads, powders, or thin films [27,28]. Given their potential for wide industrial applications, silica aerogels have been the subject of growing attention [29]. Building materials with thermal and acoustic insulation applications is currently the

* Corresponding author.
E-mail address: ahmadpour@um.ac.ir (A. Ahmadpour).

http://dx.doi.org/10.1016/j.jnoncrysol.2016.06.022
0022-3093/

main market for aerogels, though it can be applied to a wide range of other applications like adsorbents, space exploration, nuclear waste storage, drug delivery systems, batteries, sensors and catalysts [30–32]. In recent years, the adsorption of organic pollutants from wastewater by hydrophobic silica aerogel has been the subject of several studies [33–35]. Standeker et al. used silica aerogel to adsorb organic compounds such as toluene, benzene, ethyl benzene, xylene, chlorobenzene, chloroform, 1,2-dichloroethane, and trichloroethylene from water. The adsorption capacity of this adsorbent exceeded the capacity of comparable activated carbons for all toxic organic compounds [36]. Liu et al. synthesized the hydrophobic silica aerogel derived from water glass precursor as an adsorbent to remove dieldrin compound from water [34]. The adsorption of oils from pure liquid and oil–water emulsion on hydrophobic silica aerogels was investigated by Wang et al. [35]. Other compounds such as THF, DMF, acetone, CH_3CN, ethanol, AcOH, and MeOH are various aqueous pollutants adsorbed on silica aerogel. The results have shown that the adsorption capacity of silica aerogel is greater than or equal to 7 g organics tested/g adsorbent [25].

A critical parameter in the large-scale production and commercialization of silica aerogel is the preparation cost. In this study, the following three approaches have been adopted: (i) the use of inexpensive starting materials such as water glasses (sodium silicate), (ii) the development of ambient pressure drying techniques instead of conventional supercritical drying, (iii) the use of cheap solvent and gelation catalyst.

Different operational parameters such as time, temperature, pH of solution, amount of adsorbent, and agitation speed can affect the efficiency of removal in the adsorption processes, with the optimization of these parameters being vital to achieve maximum efficiency [6,7]. Statistical techniques are integral to the design, improvement and optimization of production processes. One of the statistical approaches is response surface method (RSM) [37] that draws on useful statistical and mathematical techniques to model and analyze processes in which the desirable solution is affected by several variables and optimization is required. The most well-known RSM design is the central composite design (CCD), which offers an effective method for curvature prediction of model and limiting the number of experiments. In this method, design points are categorized in three groups of center points, factorial points and star points, which are further coded at five levels ($-\alpha$, $-1, 0, 1, +\alpha$) [38,39].

To the best of authors' knowledge, there is a paucity of studies on the adsorption of naphthalene from wastewater using silica aerogel. Therefore, in this paper the effect of operational parameters such as time, pH of solution and amount of adsorbent on the removal of naphthalene from wastewater is evaluated by adopting a central composite design approach. It should be noted that in the present study, the synthesized aerogels were prepared under desirable conditions using ambient pressure drying method and low-cost materials such as industrial hexane and ordinary cationic resin.

2. Experiments

2.1. Materials

Sodium silicate solution (Si precursor, molar ratio of SiO_2:Na_2O = 1:3.3, density = 1.35), ammonia solution (32%), isopropanol and trimethylchlorosilane (TMCS), as the surface modification agent, were all purchased from Merck Company. Industrial hexane and common cationic resin were used to reduce the preparation cost. The required naphthalene was purchased from Merck as the pollutant model chemical.

2.2. Synthesis of silica aerogel

In the first step of silica aerogel preparation, the sodium silicate solution was diluted by the by distilled water to hydrolyze (sodium silicate: water (v/v) = 1:4). To replace Na^+ with H^+ in the sodium silicate structure, the cationic resin was added to the diluted solution, leading to a pH reduction of up to 2 to 3 units. Then, the ammonia solution (1 M) was added as a gelation catalytic agent and the pH of solution was increased to 4–5 units. In this step, the prepared sol was transferred to the sealed Teflon vessel and placed in an oven for 4 h at 60 °C to complete the gelation process. The aging step was performed by the immersion of hydrogel in isopropanol at 60 °C for 24 h to strengthen its structure. Similarly, to exchange the water inside gel pores, the hydrogel was maintained in hexane at 60 °C overnight. These steps were taken to replace solvent with a lower surface tension and remove water (lowering the capillary forces in the drying stage and reducing the consumption of silylating agent). Then, a mixture of TMCS/hexane (30 vol%) was used for the surface modification of hydrogel, which prompted hexane diffusion in pores and strengthened the aerogel structure. The modified gel was washed with hexane for 40 min. Finally, to produce aerogel, the wet gel was left under ambient condition overnight. The drying was completed by increasing temperature with 1 °C/min from ambient temperature up to 130 °C and keeping it constant for 30 min.

2.3. Characterization

To investigate the surface properties of aerogels, Fourier transform infrared spectroscopy (FTIR) was performed in 400–4000 cm^{-1} region by Avatar 370 (Thermo Nicolet) FT-IR spectrophotometer. The contact angle was measured to determine the hydrophobicity strength of materials by photographing the instrument. The specific surface area, cumulative pore volume and pore size distribution were determined by Brunauer, Emmett and Teller (BET) and Barrett-Joyner-Halenda (BJH) methods using BELSORP-miniII (BEL Japan, Inc.). Also, the scanning electron microscopy (LEO 1450 VP) was used to observe the microstructure and morphology of silica aerogel. The samples were prepared for SEM using gold nanoparticles as the surface coating agent. Also, the density of prepared silica aerogel was calculated by the pycnometer method. The following equation was used to measure the density:

$$d_s = \frac{(C-A) \times d_R}{(B-A)-(E-C)} \quad (1)$$

where d_s is the solid density, A is the mass of pycnometer, B is the mass of pycnometer + the mass of reference solvent, C is the mass of pycnometer + the mass of solid, E is the mass of pycnometer + the mass of reference solvent + the mass of solid and d_R is the reference solvent density (water in this study).

2.4. Liquid phase adsorption

In this experiment, the adsorbate was naphthalene with a molecular structure of $C_{10}H_8$ and molar mass of 128.17 g/mol. The kinetic studies on the adsorption of naphthalene in a batch system were carried out at 25 °C ± 1 °C in a pH of 6 ± 0.5. In these experiments, a certain amount of adsorbent (silica aerogel) was transferred to a reactor containing 13 mL of naphthalene aqueous solution at an initial concentration of 34 mg/L. In this step, 13 mL of prepared solutions with known initial concentration were transferred to a 13-mL flask, followed by the addition of certain amount of adsorbent to each flask and investigation of adsorption rate at different times.

The residual concentration of the pollutant was determined by UV–vis spectroscopy (Analyticjena, SPEKOL 1300) at the maximum absorbing wavelength (λ = 275.5 nm) [40].

The adsorption of pollutant per unit gram of adsorbent (qe, mg/g) was evaluated from the following equation:

$$q_e = \frac{(C_0-C_e) \times V}{W} \quad (2)$$

where C_0 and C_e (mg/L) are initial and equilibrium concentrations of

Table 1
Factors and their range in the CCD method for removal of naphthalene.

Factor	Name	Units	Low actual	High actual	Low coded	High coded
A	Time	min	10.00	120.00	−1.000	1.000
B	pH	–	4.00	8.00	−1.000	1.000
C	Conc. of adsorbent	g/lit	2.00	4.00	−1.000	1.000

naphthalene in an aqueous solution respectively, V (L) is the solution volume and W (g) is the mass of adsorbent.

In the pH study, HCl (1 M) and NaOH (1 M) were used to adjust the pH value using a pH-meter (HANNA pH 211) with a glass electrode.

2.5. Adsorption experiments design

Different operational parameters such as time, the initial pH of solution, the concentration of adsorbent and their interaction were investigated in the removal of naphthalene from wastewater. Subsequently, the predicted model and the optimized conditions of adsorption process were found. The range and level of parameters are presented in Table 1.

It should be noted that the required adsorbent was not prepared at one stage, meaning that it was inevitably synthesized in a two batch experiments. Thus, in the designing method, the adsorption experiments were performed in two blocks. The design of experiments (with two replications at the star and factorial points and four replications at the center point) was obtained randomly, as presented in Table 2. Possibly, since α can take any optional values, $\alpha = 1.6818$ was assumed in the present designing procedure. All experiments were performed at room temperature in an initial naphthalene concentration of 34 mg/L in water. The functional relationship between the independent variables and response was modeled by an empirical second-order

Table 2
Central composite design plan and experimental results.

Run	Block	A: time (min)	B: conc. of adsorbent (g/lit)	C: pH of solution	Removal amount (ppm)
1	Block 1	120.00	8.00	4.00	22.28
2	Block 1	10.00	8.00	2.00	15.52
3	Block 1	120.00	8.00	2.00	23.08
4	Block 1	10.00	4.00	4.00	18.08
5	Block 1	65.00	6.00	3.00	20.84
6	Block 1	10.00	8.00	2.00	16.24
7	Block 1	10.00	8.00	4.00	21.12
8	Block 1	120.00	4.00	2.00	23.11
9	Block 1	10.00	4.00	4.00	16.37
10	Block 1	10.00	4.00	2.00	14.40
11	Block 1	120.00	8.00	4.00	23.03
12	Block 1	10.00	4.00	2.00	14.27
13	Block 1	120.00	4.00	2.00	24.84
14	Block 1	120.00	4.00	4.00	25.23
15	Block 1	10.00	8.00	4.00	19.50
16	Block 1	120.00	8.00	2.00	22.83
17	Block 1	120.00	4.00	4.00	24.39
18	Block 1	65.00	6.00	3.00	22.47
19	Block 2	65.00	6.00	3.00	24.52
20	Block 2	65.00	6.00	3.00	23.22
21	Block 2	65.00	2.64	3.00	22.43
22	Block 2	0.00	6.00	3.00	Deleted
23	Block 2	65.00	6.00	1.32	21.76
24	Block 2	157.50	6.00	3.00	20.78
25	Block 2	65.00	9.36	3.00	21.44
26	Block 2	65.00	9.36	3.00	21.99
27	Block 2	0.00	6.00	3.00	Deleted
28	Block 2	65.00	6.00	1.32	19.19
29	Block 2	65.00	6.00	4.68	25.68
30	Block 2	65.00	2.64	3.00	21.73
31	Block 2	157.50	6.00	3.00	23.72
32	Block 2	65.00	6.00	4.68	24.12

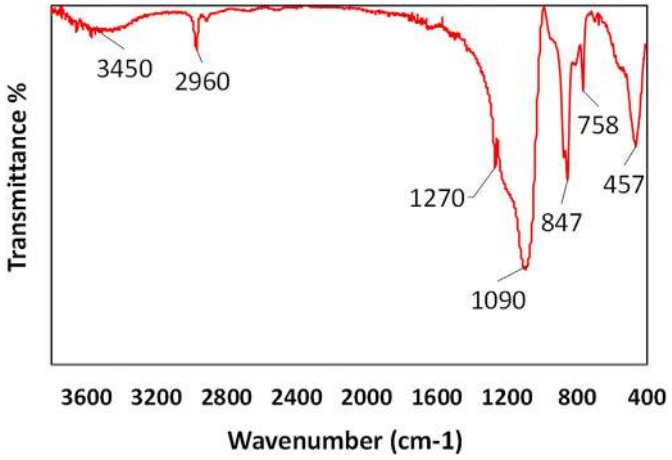

Fig. 1. FTIR spectra for hydrophobic silica aerogel.

polynomial comprising of linear, quadratic and cross-product terms to predict the optimum conditions, which can be expressed according to the following equation:

$$Y = \beta_0 + \sum_{i=1}^{k}\beta_i x_i + \sum_{i=1}^{k}\beta_{ii}x_i^2 + \sum_{i\le j}^{k}\sum_{j}^{k}\beta_{ij}.x_i.x_j + \ldots + \varepsilon \quad (3)$$

where, β_0 is the constant coefficient, β_i is the linear coefficient, β_{ii} is the quadratic coefficient and β_{ij} is the interactive coefficient [41].

3. Results and discussion

3.1. Characterization of prepared silica aerogel

The Fourier transform infrared spectroscopy (FTIR) of the prepared silica aerogel is presented in Fig. 1. Peaks at 1090 cm^{-1}, 758 cm^{-1} and 457 cm^{-1} can be attributed to the symmetric, asymmetric and bending of Si-O-Si bonds respectively, which indicate the network structure of silica aerogel. Given the surface modification with TMCS, the peaks at 847 cm^{-1}, 1260 cm^{-1} and 2960 cm^{-1} confirmed the presence of methyl groups on the aerogel surface. The weakened peak centered at 3450 cm^{-1} corresponds to the OH groups and physisorbed

Fig. 2. Contact angle photograph of water droplet on hydrophobic surface of silica aerogel.

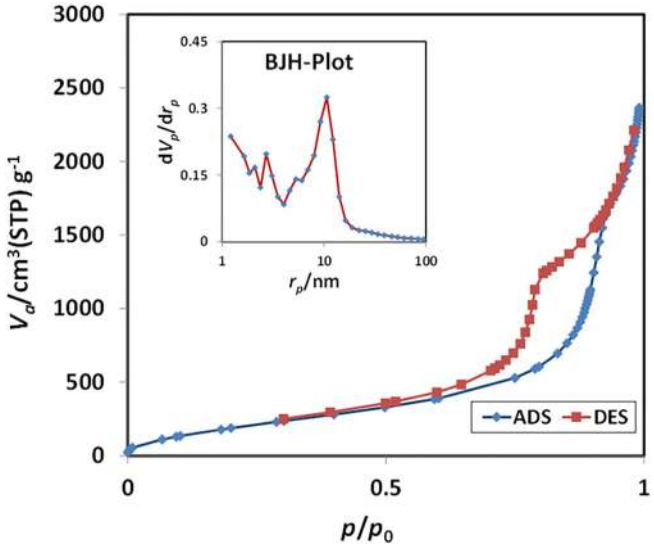

Fig. 3. N2 adsorption/desorption isotherms and pore size distribution plots for hydrophobic silica aerogel.

water molecules, thus verifying the desirable hydrophobicity of surface [42,43].

The contact-angle photograph of the water droplet on the aerogel surface is presented in Fig. 2. The high contact angle exhibits high hydrophobic strength and desirable surface modification. The contact angle was obtained at 145°, which confirmed the presence of methyl group (hydrophobic agent) bonded onto the surface [34].

Adsorption and desorption isotherms and pore-size distribution of aerogel are shown in Fig. 3. The nitrogen adsorption following type-IV isotherm indicates high mesoporosity in the structure of aerogel. The presence of hysteresis loop is due to the capillary condensation in the mesopores. Furthermore, major pores with a diameter of around 10.65 nm verified the mesopore structure. BET values of surface area, pore volume and mean pore diameter were 823 m^2/g, 3.63 cm^3/g and 17.67 nm respectively [44,45]. (See Table 3).

To investigate the structure and morphology of silica aerogel at high magnification, the scanning electron microscope was employed. As shown in Fig. 4, the porous structure with a particle size <100 nm is verified [46].

3.2. Design experiment

The results of experimental design of adsorption tests are shown in ANOVA table. The significance of the model and terms are determined by statistical parameters such as F-value, *P*-value, lack of fit, coefficient of determination (R^2) and adjusted coefficient of determination ($R^2_{adj.}$). If *P*-value is <0.05, the term will be significant but higher F-value provides an accurate prediction of experimental data. The lack of fit parameter corresponds to the fitting of the model with the non-significant lack of fit providing a desirable indication of the model fitness. The R^2 parameter represents the strength of correlation between experimental data and the statistical model whereas added number of terms increased R^2. On the other hand, the value of $R^2_{adj.}$ is increased by removing the non-significant terms. The coefficient of variation (C·V) and adequate precision are other parameters that must be determined. If the C·V value is <10, the proposed model will be reproducible. The adequate precision is a signal to noise ratio and a measure ratio of the predicted values to the average prediction error. In which ratio >4 is acceptable [47–49].

Table 3
Physical properties of hydrophobic silica aerogel.

Characterization results	
Specific surface area (m^2/g)	823
Total pore volume (cm^3/g)	3.63
Mean pore diameter (nm)	17.67
Density (g/cm^3)	0.18
Contact angle (°)	145

The ANOVA table was prepared using the backward elimination method for the model improvement by removing the insignificant terms, as shown in Table 4. The empirical quadratic model was estimated by RSM where R^2 and $R^2_{adj.}$ were equal to 0.904 and 0.877 respectively (Eq. (4)). The significance of the model was confirmed by the F-value of 34.37. Also, the insignificance of lack of fit relative to the pure error represented the fitness of the model properly. Also, the estimated C·V and adequate precision of the related model were 5.09 and 19.28 respectively. In the adsorption of naphthalene onto the silica aerogel, A, C, AB, AC, A^2 are significant model terms. Considering the F-values, it can be concluded that time is the most effective parameter in the adsorption process.

$$Removalamount = 22.39 + 3.29A + 0.06B + 1.12\,C - 0.98AB - 0.85AC - 2A^2 \quad (4)$$

The normal probability plot is a helpful instrument indicating the normal distribution of residuals. In this plot, the points follow a straight line. As shown in Fig. 5, the plot confirms the normal distribution of errors with a mean zero (and constant but unknown variance as the underlying assumption of the analysis) [50].

The residuals versus predicted response values plot was employed to investigate the assumption of constant variance. As observed in Fig. 6, there is a random dispersion of points above and below the x-axis between ±3.0, which verify the adequacy and reliability of the proposed models [51].

In this study, 3D plots are utilized to present the simultaneous effect of two indepndent variables and their interactions. Therefore, two factors are considered as study variables and other factors are treated as constant values, with the interaction of varible factors being evaluated on the response value. In fact, these plots show the effect of one factor on the response value at different levels of other factors. Also, it should be noted that the 3D plots were achieved based on the proposed model.

Since there were 3 factors in the experimental design, 3 types of interaction can be dsitinguished. As noted earlier, the interaction of AB and AC were significant, and their effects on the adsorption process of naphthalen are shown in Fig. 7. According to Fig. 7a, the naphthalene removal process was increased rapidly at the outset of the reaction, and subsequently the adsorption rate was marginally increased over time and reached the equilibrium. The dramatic rise of removal efficiency in the initial stages indicated the presence of numerous readily accessible sites. An increase in the adsorbed volume over time is due to greater contact between the sorbent surface and naphthalene molecules.

As for the pH of solution, the results show that a medium pH level does not have any significant effect on the removal effeciency of naphtalene. To investigate the pH effect, the octanol-water partition coefficient (*log K*) must be evaluated for naphthalene molecule. Basically, $log\ K_{oct/wat}$ is defined as the ratio of component concentration in a mixture of two immiscible phases at equilibrium, which depends on the solubility of each phase. The high value of $log\ K_{oct/wat}$ represents the greater tendency of molecule to the hydrophobic media [52]. In the process of naphthalene adsorption from wastewater, the silica aerogel has a hydrophobic surface with a hydrophilic adsorption media (aqueous solution). Since the value of log $K_{oct/wat}$ for the naphthalene molecule is 3.30 [53], its molecules can be conveniently incorporated in hydrophobic media like silica aerogel at all pH ranges. Hence, the variation of pH

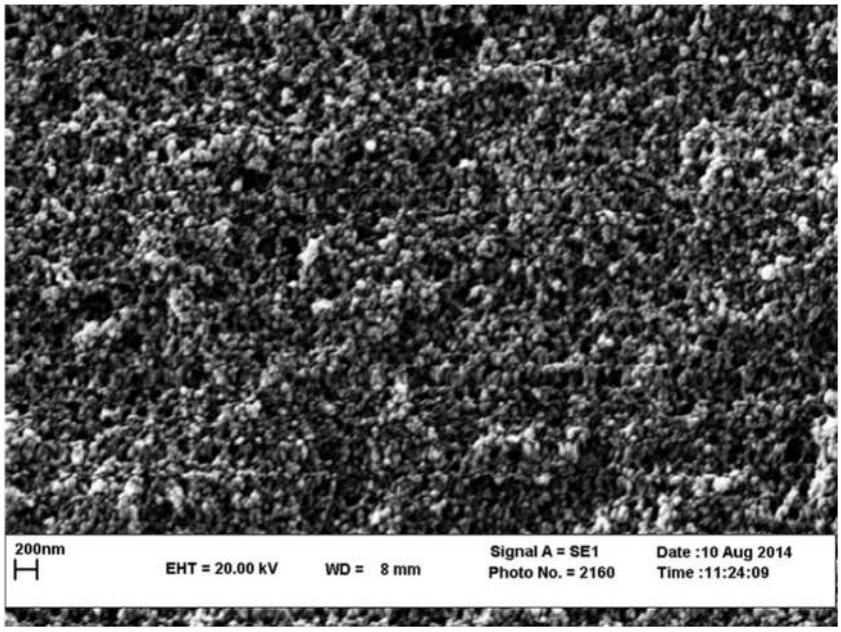

Fig. 4. SEM image of hydrophobic silica aerogel.

did not have any effect on the removal of naphthalene, which was consistent with the ANOVA results. On the other hand, the variation in the amount of removal with respect to time axis was approximately identical to AB interaction in a 3D plot, as presented in Fig. 7b. The amount of adsorbent was another significant variable in the adsorption of naphthalene on silica aerogel because an increase in the adsorbent created greater adsorption sites for naphthalene molecules As shown in Fig. 7.b, the amount of naphthalene removal changed linearly with the adsorbent concentration, but its effect declined gradually over time.

3.3. Optimization

One important goal of the experimental design is the optimization of process. In this research, the goal was to reach maximum removal amount of naphthalene from wastewater using silica aerogel. DESIGN EXPERT software allows measuring the optimum value for the desired purpose. Thus, for any variable and response value, several alterantives such as maximum, minimum, target, within range, none (for responses only) and exact values (factors only) can be assumed. The numerical optimization seeks to find a point that can maximize the desirability function. Simply put, desirability is a mathematical method to find the optimum condition. The goal of optimization is to find a favorable set of conditions that can fulfill all the goals rather than reach the desirability value of 1.0.

For this purpose, the operational variables were set at "within range" and the "maximum value" was selected for the response. The result of optimization is presented in Table 5. It is clear that under optimized condition, the experimental response value is close to the pridicted response value, with the results demonstrating the validation of the proposed model. Also, it should be noted that the optimized condition is a statistical output regardless of the economical issues, whereas its effects need to be exmained in real-life process.

Table 4
ANOVA results for response surface reduced quadratic model.

Source	Sum of squares	df	Mean square	F-value	*P*-value	
Block	32.55	1	32.55			
Model	241.45	6	40.24	34.37	<0.0001	Significant
A	179.19	1	179.19	153.06	<0.0001	
B	0.10	1	0.10	0.089	0.7689	
C	34.27	1	34.27	29.27	<0.0001	
AB	15.23	1	15.23	13.01	0.0016	
AC	11.51	1	11.51	9.83	0.0048	
A^2	48.35	1	48.35	41.30	<0.0001	
Residual	25.76	22	1.17			
Lack of fit	9.14	7	1.31	1.18	0.3706	Not significant
Pure error	16.61	15	1.11			
Cor total	299.75	29	32.55			

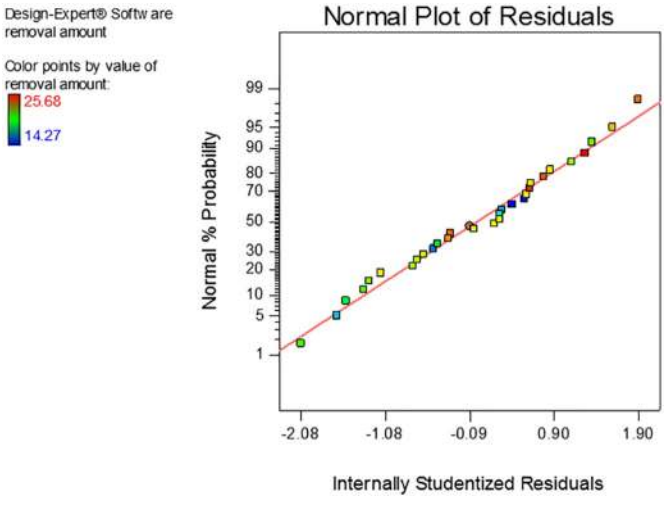

Fig. 5. The studentized residual and normal % probability plot.

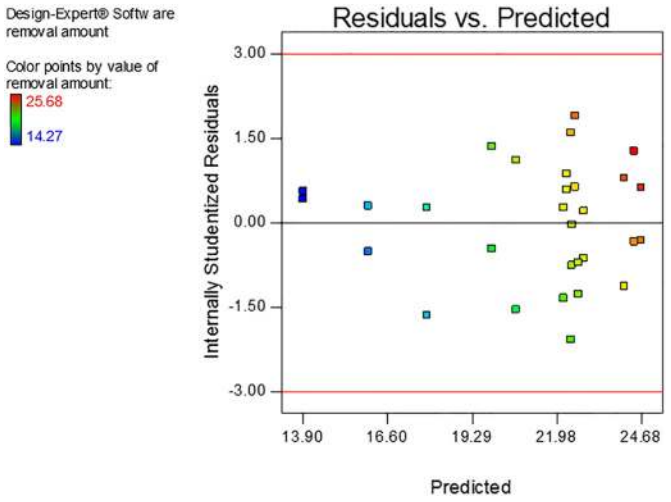

Fig. 6. Studentized residual versus predicted of removal of naphthalene.

3.4. Kinetic study

The prediction of adsorption rate is an important factor in the design of adsorption process, because adsorbate residence time and reactor dimensions are determined by system's kinetics. The adsorption mechanism has been determined in various kinetic models. In the present study, Lagergren's pseudo-first-order and Ho's pseudo-second-order expressions were used to investigate the adsorption kinetic. Lagergren's equation has been used for the adsorption of different pollutants onto many adsorbents, but it is especially suitable for the initial times of the process [54]. It is obvious that in Lagergren's equation, the kinetic constant is achieved by plotting $\log(q_e - q_t)$ versus t.

$$log(q_e - q_t) = logq_e - \frac{K_1 t}{2.303} \quad (5)$$

where $q_t$and q_e are respectively the amount of adsorption at time t and equilibrium (mg/g) and K_1 is the pseudo-first-order rate constant (min^{-1}).

Ho's model is often used to predict the kinetic of process when the chemical bond is formed between the solute and solid in the adsorption by various forces using the sharing or exchange of electrons as covalent forces [55]. In accordance with the following equation, q_e and K_2 can be measured by plotting t/q_t versus t.

$$\frac{t}{q_t} = \frac{1}{K_2 q_e^2} + \frac{t}{q_e} \quad (6)$$

Table 5
Model validation of removal of naphthalene at optimized condition.

Optimized condition				Removal value of naphthalene (mg/L)	
Time (min)	pH	Conc. of adsorbent (g/L)	Desirability	Experimental	Predicted
120	4	4	0.932	24.68	24.9

where K_2 is the rate constant of second order adsorption (g/mg·min). The slope and intercept in t/q_t versus t plots (figures are not shown) were used to calculate the second order rate constant K_2.

Kinetic experiments were carried out under following conditions ($pH = 6$, sorbent = 2 g/L and time = 5 to 120 min). The pseudo second-order rate constant (K_2), correlation coefficients (R^2) and experimental and calculated uptake capacities (q_e) are presented in Table 6. As can be seen, it is obvious that the coefficient of determination in Ho's equation is larger than that of Lagergren's equation. Moreover, the predicted q_e value in the Ho's model is more consistent with the experimental q_e. This model was utilized to adsorb organic compounds from the aqueous solution and to predict adsorption process at low concentration. Probably, the covalent bond was the result of hydrophobic surface of silica aerogel and non-polar nature of naphthalene.

4. Conclusion

In this study, hydrophobic silica aerogel was synthesized using sodium silicate precursor and ambient pressure drying method. Also, the industrial solvent and common cationic resin were used to reduce the preparation cost. The results of characterization revealed that the use of these materials had no considerable effect on the properties of silica aerogel such as specific surface area, pore volume, density and hydrophobicity.

This study was the first attempt in which the prepared silica aerogel was used to remove naphthalene from water media. To optimize adsorption parameters, the CCD experimental design method was used with factors such as time, pH of solution and amount of adsorbent being assumed as operational variables. ANOVA results verified appropriate statistical parameters such as coefficient of determination ($R^2 = 0.903$), adjusted coefficient of determination ($R^2_{adj.} = 0.877$), coefficient of variation (5.09) and adequate precision (19.23). In the end, a second order model was proposed. The results indicated that time and amount of adsorbent were significant variables, though it was not the case for the pH of solution. The optimized values of time (120 min), pH of solution ($pH = 4$) and amount of adsorbent (4 g/L) were obtained. The consistency between the predicted and experimental results under this condition verified the validity of the optimal point achieved in this study.

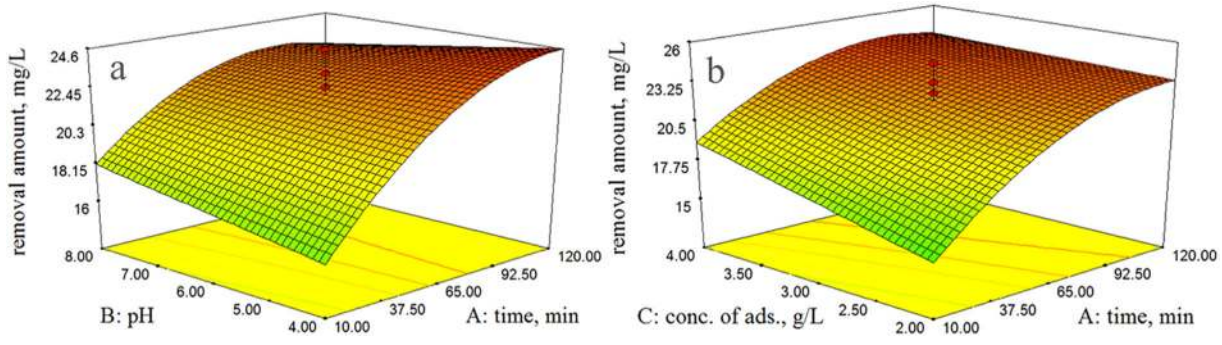

Fig. 7. 3D plots obtained from proposed model for removal of naphthalene. a) time-pH interaction, b) time-conc. of ads. interaction.

Table 6
Kinetic parameters for Ho model and Lagergren model.

Ho's pseudo-second-order				Lagergren's pseudo-first-order			
q_e (mg/g)		R^2	K_2 (g/mg·min)	q_e (mg/g)		R^2	K_1 (1/min)
Experimental	Predicted			Experimental	Predicted		
0.0375	0.9413	12.25	6.24	0.014	0.9985	12.25	12.77

Reference

[1] A.C. Ion, I. Ion, A. Culeţu, Adsorption of naphthalene onto carbonic nanomaterial graphitic nanoplatelets in aqueous solutions, UPB Sci. Bull. Ser. B 73 (2011) 55–66.
[2] K. Skupinska, I. Misiewicz, T. Kasprzycka-Guttman, Polycyclic aromatic hydrocarbons: physicochemical properties, environmental appearance and impact on living organisms, Acta Pol. Pharm. 61 (2004) 233–240.
[3] J.-I. Park, J.-K. Lee, J. Miyawaki, S.-H. Yoon, I. Mochida, Catalytic oxidation of polycyclic aromatic hydrocarbons (PAHs) over SBA-15 supported metal catalysts, J. Ind. Eng. Chem. 17 (2011) 271–276.
[4] S. Sener, A. Ozylmaz, Adsorption of naphthalene onto sonicated talc from aqueous solutions, Ultrason. Sonochem. 17 (5) (2010) 932–938.
[5] H. Karyab, M. Yunesian, S. Nasseri, A.H. Mahvi, R. Ahmadkhaniha, N. Rastkari, R. Nabizadeh, Polycyclic aromatic hydrocarbons in drinking water of Tehran, Iran, J. Environ. Health. Sci. Eng. 11 (2013) 25.
[6] O. Gok, A.S. Ozcan, A. Ozcan, Adsorption kinetics of naphthalene onto organo-sepiolite from aqueous solutions, Desalination 220 (2008) 96–107.
[7] S.E. MORADI, Naphthalene removal from water by novel mesoporous carbon nitride adsorbent, Chem. Biochem. Eng. Q. 27 (2013) 365–372.
[8] M. Usman, D. Li, R. Razzaq, M. Yaseen, C. Li, S. Zhang, Novel MoP/HY catalyst for the selective conversion of naphthalene to tetralin, J. Ind. Eng. Chem. 23 (2015) 21–26.
[9] M. Norouzi Rad, Adsorption Behavior of Naphthalene Onto Organoclay in Aqueous Solution, Department of Civil and Environmental Engineering, Northeastern, Boston, Massachusetts, 2010 85.
[10] L.P. Ramteke, P.R. Gogate, Treatment of toluene, benzene, naphthalene and xylene (BTNXs) containing wastewater using improved biological oxidation with pretreatment using Fenton/ultrasound based processes, J. Ind. Eng. Chem. 28 (2015) 247–260.
[11] M.-H. Yuan, C.-Y. Chang, J.-L. Shie, C.-C. Chang, J.-H. Chen, W.-T. Tsai, Destruction of naphthalene via ozone-catalytic oxidation process over Pt/Al2O3 catalyst, J. Hazard. Mater. 175 (2010) 809–815.
[12] O.A. Ali, S.J. Tarek, Removal of polycyclic aromatic hydrocarbons from Ismailia Canal water by chlorine, chlorine dioxide and ozone, Desalin. Water Treat. 1 (2009) 289–298.
[13] A. Sharma, B.-K. Lee, Adsorptive/photo-catalytic process for naphthalene removal from aqueous media using in-situ nickel doped titanium nanocomposite, J. Environ. Manag. 155 (2015) 114–122.
[14] H. Shi, T. Zhang, H. Wang, X. Wang, M. He, Photocatalytic conversion of naphthalene to a-naphthol using nanometer-sized TiO2, Chin. J. Catal. 32 (2011) 46–50.
[15] C. Lin, L. Gan, Z.-L. Chen, Biodegradation of naphthalene by strain *Bacillus fusiformis* (BFN), J. Hazard. Mater. 182 (2010) 771–777.
[16] Y.-I. Chang, H.-P. Cheng, S.-H. Lai, H. Ning, Biodegradation of naphthalene in the oil refinery wastewater by enriched activated sludge, Int. Biodeterior. Biodegrad. 86 (Part C) (2014) 272–277.
[17] J. Wang, Z. Chen, B. Chen, Adsorption of polycyclic aromatic hydrocarbons by graphene and graphene oxide nanosheets, Environ. Sci. Technol. 48 (2014) 4817–4825.
[18] E.M.O. Kaya, A.S. Ozcan, O. Gok, A. Ozcan, Adsorption kinetics and isotherm parameters of naphthalene onto natural- and chemically modified bentonite from aqueous solutions, Adsorption 19 (2013) 879–888.
[19] B. Cabal, T. Budinova, C.O. Ania, B. Tsyntsarski, J.B. Parra, B. Petrova, Adsorption of naphthalene from aqueous solution on activated carbons obtained from bean pods, J. Hazard. Mater. 161 (2009) 1150–1156.
[20] Z. Pei, L. Li, L. Sun, S. Zhang, X.-q. Shan, S. Yang, B. Wen, Adsorption characteristics of 1,2,4-trichlorobenzene, 2,4,6-trichlorophenol, 2-naphthol and naphthalene on graphene and graphene oxide, Carbon 51 (2013) 156–163.
[21] M.S. Shafeeyan, W.M.A.W. Daud, A. Shamiri, N. Aghamohammadi, Adsorption equilibrium of carbon dioxide on ammonia-modified activated carbon, Chem. Eng. Res. Des. 104 (2015) 42–52.
[22] B. Dou, J. Li, Y. Wang, H. Wang, C. Ma, Z. Hao, Adsorption and desorption performance of benzene over hierarchically structured carbon-silica aerogel composites, J. Hazard. Mater. 196 (2011) 194–200.
[23] M.H. Givianrad, M. Rabani, M. Saber-Tehrani, P. Aberoomand-Azar, M. Hosseini Sabzevari, Preparation and characterization of nanocomposite, silica aerogel, activated carbon and its adsorption properties for Cd (II) ions from aqueous solution, J. Saudi Chem. Soc. 17 (2011) 329–335.
[24] A. Venkateswara Rao, N.D. Hegde, H. Hirashima, Absorption and desorption of organic liquids in elastic superhydrophobic silica aerogels, J. Colloid Interface Sci. 305 (2007) 124–132.
[25] H.-x. Shi, J.-t. Cui, H.-m. Shen, H.-k. Wu, Preparation of silica aerogel and its adsorption performance to organic molecule, Adv. Mater. Sci. Eng. 2014 (2014) 8.
[26] S. Kumar Rajanna, M. Vinjamur, M. Mukhopadhyay, Mechanism for formation of hollow and granular silica aerogel microspheres from rice husk ash for drug delivery, J. Non-Cryst. Solids 429 (2015) 226–231.
[27] S.D. Bhagat, K.-T. Park, Y.-H. Kim, J.-S. Kim, J.-H. Han, A continuous production process for silica aerogel powders based on sodium silicate by fluidized bed drying of wet-gel slurry, Solid State Sci. 10 (2008) 1113–1116.
[28] P.B. Sarawade, D.V. Quang, A. Hilonga, S.J. Jeon, H.T. Kim, Synthesis and characterization of micrometer-sized silica aerogel nanoporous beads, Mater. Lett. 81 (2012) 37–40.
[29] A.A. Michel, N. Leventis, M.M. Koebel, Aerogels Handbook, 1 ed. Springer-Verlag New York, 2011.
[30] L.G. Jyoti, J. In-Keun, P. Hyung-Ho, K. Eul Son, Y.N. Digambar, Silica aerogel: synthesis and applications, J. Nanomater. 2010 (2010) 1–11.
[31] A. Du, B. Zhou, Z. Zhang, J. Shen, A special material or a new state of matter: a review and reconsideration of the aerogel, Materials 6 (2013) 941–968.
[32] T. Mehling, I. Smirnova, U. Guenther, R.H.H. Neubert, Polysaccharide-based aerogels as drug carriers, J. Non-Cryst. Solids 355 (2009) 2472–2479.
[33] K. Wormeyer, I. Smirnova, Adsorption of CO2, moisture and ethanol at low partial pressure using aminofunctionalised silica aerogels, Chem. Eng. J. 225 (2013) 350–357.
[34] H. Liu, W. Sha, A.T. Cooper, M. Fan, Preparation and characterization of a novel silica aerogel as adsorbent for toxic organic compounds, Colloids Surf. A Physicochem. Eng. Asp. 347 (2009) 38–44.
[35] D. Wang, E. McLaughlin, R. Pfeffer, Y.S. Lin, Adsorption of oils from pure liquid and oil-water emulsion on hydrophobic silica aerogels, Sep. Purif. Technol. 99 (2012) 28–35.
[36] S. Standeker, Z. Novak, Z. Knez, Adsorption of toxic organic compounds from water with hydrophobic silica aerogels, J. Colloid Interface Sci. 310 (2007) 362–368.
[37] C.M. Douglas, G.C. Runger, Applied Statistics & Probability for Engineers, 5 ed., 2011.
[38] E.A. Diler, R. Ipek, Main and interaction effects of matrix particle size, reinforcement particle size and volume fraction on wear characteristics of Al-SiCp composites using central composite design, Compos. Part B 50 (2013) 371–380.
[39] T. Eppinger, G. Wehinger, M. Kraume, Parameter optimization for the oxidative coupling of methane in a fixed bed reactor by combination of response surface methodology and computational fluid dynamics, Chem. Eng. Res. Des. 92 (2013) 1693–1703.
[40] C.O. Ania, B. Cabal, C. Pevida, A. Arenillas, J.B. Parra, F. Rubiera, J.J. Pis, Effects of activated carbon properties on the adsorption of naphthalene from aqueous solutions, Appl. Surf. Sci. 253 (2007) 5741–5746.
[41] A. Nazari, M. Mirjalili, N. Nasirizadeh, S. Torabian, Optimization of nano TiO2 pretreatment on free acid dyeing of wool using central composite design, J. Ind. Eng. Chem. 21 (2015) 1068–1076.
[42] C. Kim, J. Yoon, H. Hwang, Synthesis of nanoporous silica aerogel by ambient pressure drying, J. J. Sol. Gel Sci. Technol. 49 (2009) 47–52.
[43] P.B. Sarawade, J.-K. Kim, A. Hilonga, H.T. Kim, Production of low-density sodium silicate-based hydrophobic silica aerogel beads by a novel fast gelation process and ambient pressure drying process, Solid State Sci. 12 (2010) 911–918.
[44] S.K. Hong, M.Y. Yoon, H.J. Hwang, Synthesis of spherical silica aerogel powder by emulsion polymerization technique, J. Ceram. Process. Res. 13 (2012) 145–148.
[45] U.K.H. Bangi, I.-K. Jung, C.-S. Park, S. Baek, H.-H. Park, Optically transparent silica aerogels based on sodium silicate by a two step sol–gel process and ambient pressure drying, Solid State Sci. 18 (2013) 50–57.
[46] S. He, D. Huang, H. Bi, Z. Li, H. Yang, X. Cheng, Synthesis and characterization of silica aerogels dried under ambient pressure bed on water glass, J. Non-Cryst. Solids 410 (2015) 58–64.
[47] V. Mahmoodi, J. Sargolzaei, Optimization of photocatalytic degradation of naphthalene using nano-TiO2/UV system: statistical analysis by a response surface methodology, Desalin. Water Treat. 52 (2013) 6664–6672.
[48] J. Zolgharnein, M. Bagtash, N. Asanjarani, Hybrid central composite design approach for simultaneous optimization of removal of alizarin red S and indigo carmine dyes using cetyltrimethylammonium bromide-modified TiO2 nanoparticles, J. Environ. Chem. Eng. 2 (2014) 988–1000.
[49] E. Geravand, Z. Shariatinia, F. Yaripour, S. Sahebdelfar, Synthesis of copper-silica nanosized catalysts for 2-butanol dehydrogenation and optimization of preparation parameters by response surface method, Chem. Eng. Res. Des. 96 (2015) 63–77.
[50] R. Gheshlaghi, J.M. Scharer, M. Moo-Young, C.M. Douglas, Application of statistical design for the optimization of amino acid separation by reverse-phase HPLC, Anal. Biochem. 383 (2008) 93–102.
[51] K. Mahdi, R. Gheshlaghi, G. Zahedi, A. Lohi, Characterization and modeling of a crude oil desalting plant by a statistically designed approach, J. Pet. Sci. Eng. 61 (2008) 116–123.

[52] P. Molyneux, Octanol/water partition coefficients Kow: a critical examination of the value of the methylene group contribution to log Kow for homologous series of organic compounds, Fluid Phase Equilib. 368 (2014) 120–141.
[53] J. Sangster, Octanol-water partition coefficients of simple organic compounds, J. Phys. Chem. Ref. Data 18 (1989) 1111–1229.
[54] R.-L. Tseng, F.-C. Wu, R.-S. Juang, Characteristics and applications of the Lagergren's first-order equation for adsorption kinetics, J. Taiwan Inst. Chem. Eng. 41 (2010) 661–669.
[55] Y.-S. Ho, Review of second-order models for adsorption systems, J. Hazard. Mater. 136 (2006) 681–689.